Influence of Curing Media on Properties of Alkali-treated Paddy Straw-based Lightweight Geopolymer Composites

Nidhya Rathinavel[a], Arun Murugesan[a], Sivasubramanian Ramanathan[b], Muthukaruppan Alagar[c], and Abdul Aleem Mohamed Ismail[a,*], Hitesh Panchal [d], Naveen Kumar Gupta [e],

[a]Engineering Materials Laboratory, Department of Civil Engineering, PSG Institute of Technology and Applied Research, Neelambur, Coimbatore - 641 062, India.

[b]Electrochemical Sensors and Energy Materials Lab, PSG Institute of Advanced Studies, Coimbatore 641004

[c]Polymer Engineering Laboratory, PSG Institute of Technology and Applied Research, Neelambur, Coimbatore - 641 062, India.

d Assistant Professor, Mechanical Engineering Department, Government Engineering College patan, Gujarat, India.

e Department of Mechanical Engineering, GLA University, Mathura, India.

Abstract

This research mainly focused on studying the influence of various curing media on the properties of lightweight geopolymer composites. Here, Ground Granulated Blast furnace Slag (GGBS), Paddy straws, and the combination of sodium silicate and sodium hydroxide at the ratio of 2.5:1 were used to produce geopolymer composites. For this experiment, two different parameters, i.e., variation of paddy straw (0%, 5%, 10%, 15%, and 20%) and variation of curing media (Intermittent, Heat, and Saline water), were chosen. The compressive strength of a 20% addition of paddy straw is dramatically reduced by 88.6%, while the density is reduced to 40.42%. Maximum flexure and

tensile strength were noted as 65.11% and 45.5%, respectively, for the 15% addition of paddy straw. An interesting fact found from the samples cured under Saline water enhanced the overall compressive strength, tensile and flexural strength by 12.85%, 45.5%, and 21.2%, respectively, compared to other two curing media.

KEYWORDS Lightweight Geopolymer, Saline Curing, Intermittent Curing, Heat Curing, Alkali treated Paddy Straw.

INTRODUCTION

The current scenario needs eco-friendly and environmentally sustainable construction materials to preserve the earth by controlling the emission of greenhouse gases. This goal can be achieved by converting waste materials from agricultural, thermal, and steel industries into alternative construction materials. The present work provides an overview of efficiently disposing waste materials from agro and steel industries. Paddy straw, a byproduct of rice production found all over the world. Production is increasing rapidly with an increase in population demand. The farmers choose the open burning method, which is cheap to dispose of paddy straw. This process produces large amounts of organic, inorganic, toxic, and greenhouse gases in the atmosphere [1, 2]. Paddy straw has been studied extensively for its potential as a natural fibre reinforcement. Renewable paddy straw fibres possess a high positive impact on the cementitious reinforced material[3-5]. Previous research has proven that alkali-treated paddy straw exhibits better binding properties than that untreated rice straw. Alkali treatment of paddy straw eliminates the organic compounds and low molecular weight hemicellulose, thereby improving the fibre strength and efficient bonding with matrixes [6-8]. The recent trend mainly focuses on developing lightweight building materials and renewable sources for an eco-friendly and sustainable environment. Currently, lightweight building

materials are used for different applications, viz., thermal insulation, sound insulation, and lightweight structural parts. It was already established that wood or any other natural fibres are used as reinforcing material, which contributes to reducing the weight and, in turn, results from the composites with lower density and lightweight [9].

In the future, using geopolymer as a replacement material for cement will reduce CO_2 to 80% around the world [10-15]. Utilizing alumino-silicate materials wasted from various industries like iron manufacturing and thermal power plants can be used as the binding media to produce composites for construction. GGBS, metakaolin, rice husk ash, and fly ash are examples of aluminosilicate materials that can be activated with alkaline solutions to produce geopolymer composites. The process of geo-polymerization mainly depends on the presence of aluminosilicate minerals and alkali-activating liquids[16]. Geo-polymerization occurs between silica and alumina in an alkaline solution, producing Si-O-Al-O linkage with three-dimensional cross-linked network structures. Unlike cement matrix, geopolymer composites undergo polycondensation of silicate and alumina in the presence of an alkaline solution. Fly ash and metakaolin-based aluminate produces sodium aluminosilicate hydrate gel, whereas GGBS produces calcium aluminosilicate hydrate gel. Though the geopolymer with metakaolin attains maximum strength than other aluminosilicate materials, their applications are limited due to their higher water absorption, which leads to rheological problems. Among the aluminosilicate materials, fly-ash-based composites possess better durability; whereas GGBS-based composites attain high early high strength with better acid resistance [13, 16].

At present, there are many precast geopolymeric materials available in the market, however, heat curing limits its application in construction industries. However, research related to geopolymer is in progress to study their performance under different curing media to replace port-land cement products to the extent possible [17-20]. Recent research states that physical, mechanical, and durability

properties are directly related to alkali activator, fineness, mineral composition, the source of aluminosilicate material used, alkali binder ratio, and concentration of alkaline liquid and different curing regimes [21-23]. Further, the study states that alkali activation activates aluminosilicate binder and alkaline material to produce the hardened product. It is found from previous research that the calcium content present in the aluminosilicate is responsible for hardening at an early age. Alkali activation is activating geopolymeric binders to obtain hardened composite materials. Calcium in aluminosilicate materials causes composites to harden at ambient temperature, however low calcium binder composites require heat curing. [24-26]. GGBS and fly ash combination possess more compressive strength than other aluminosilicate materials [27].

On the other hand, more research is needed on curing geopolymers in saline water. However, from some research, fly ash mixed with a small amount of salt significantly impacts the strength and properties [28]. It is also evident that saline curing of samples was done after they were partially cured under air and heat. Few literatures provide information about geopolymer curing under normal and saline water. The presence of abundant Na+ and cation (Ca+) in the surrounding saline solution is prone to chemical leaching and increases the reaction rate. It leads to early hardening with high strength. Due to its less porosity, saline-cured geopolymers possess very low sorptivity values [29, 30].

Even though the curing of geopolymer is an important influencing factor, which governs the polymerization and is responsible for the hardening of structure, only a few literatures described it. Hence, this research intensely focuses on studying the influence of different curing media on the properties of lightweight geopolymer composites.

RESEARCH SIGNIFICANCE

An Alternative to heat curing is the most searched solution for the geopolymer application. Only very few literatures established different curing conditions. From the literature survey, an exciting fact was found that the saline environment had a highly positive impact on geopolymer, whereas it degraded the performance of cement. Hence this study included saline water curing as one of the curing media, along with heat and intermittent curing. The investigation's findings are novel and will be very helpful for a better understanding of how the material behaves under different curing media during the production stage.

EXPERIMENTAL INVESTIGATION

Materials

The raw paddy straw was gathered from a paddy field at Coimbatore, Tamil Nadu, India. The gathered paddy straw was treated with an alkaline solution to remove the impurities. The process of alkali treatment is described in the following paragraphs. The GGBS supplied by precision scientific co; Coimbatore was used as the primary binding material as it possesses high aluminosilicate minerals. The elemental composition and morphology of treated paddy straw and GGBS were obtained using energy dispersive X-ray (EDX) spectral analysis in conjunction with scanning electron microscopy (SEM), and the results are shown in Tables 1 and 2. Using an electron microscope with a 5kV electron beam, the SEM images of GGBS and treated paddy straw were captured and displayed in Figure. 1a, b. It showed that the treated paddy straw has a rough surface, which helps bind with surrounding geopolymer composites. The NaOH treatment removes the excess oily substances, waxes, extractives, and amorphous constituents[31]. Previous research studies substantiated that the same alkali-treated paddy straw fibre has greater roughness than

untreated paddy straw [32,33]. SEM images obtained for GGBS indicate the presence of flaky and crystalline shape particles.

In this research, the alkaline activator obtained from the combination of sodium silicate (Na_2Sio_3) and sodium hydroxide (NaOH) at 8M with a ratio of 2.5:1 was used. Sodium silicate was bought in liquid form based on the chemical requirement viz., specific gravity as 1.52, Na_2O as 14.6%, SiO_2 as 29.3%, and water as 55.9%, whereas NaOH was bought in the form of pellets with a purity of 98%. NaOH pellets were dissolved in distilled water to create the NaOH solutions to create the appropriate molarity.

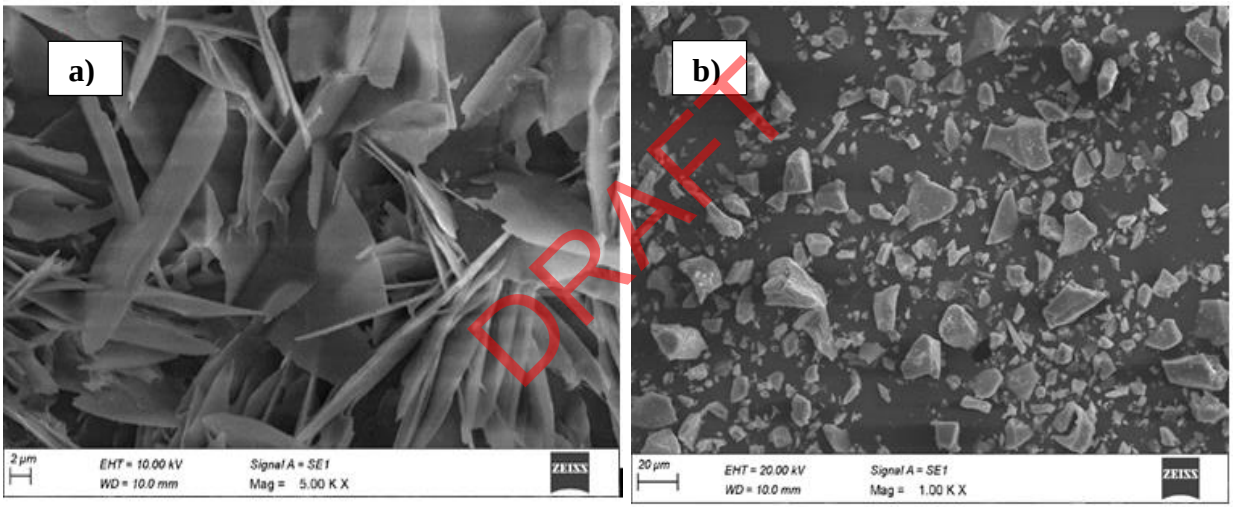

FIGURE 1 a, b. SEM Images of alkali-treated paddy straw and GGBS

TABLE 1 Elemental Composition of treated paddy straw

Element	Weight %	Atomic %	Error %
C	8.80	13.96	9.63
N	7.03	9.55	8.46
O	32.50	38.70	6.41
Na	30.49	25.26	5.69

Si	8.15	5.52	7.03
Cl	13.04	7.01	9.18

TABLE 2 Elemental Composition of GGBS

Element	Weight %	Atomic %	Error %
O	39.19	57.38	10.06
Mg	3.41	3.29	7.92
Al	8.90	7.72	5.65
Si	15.92	13.27	4.89
Nb	2.12	0.53	6.9
Ca	30.47	17.81	2.15

Alkali treatment

The raw paddy straws were cut into small pieces by shredding. The shredded paddy straw was soaked in the alkaline solution (5% NaOH) for 4h. Excess alkalinity was removed by washing alkaline paddy straw with water until the pH reached 7. The treated paddy straw was dried entirely in a hot air oven for 24 h at 45 ^{0}C to remove the moisture content. The process of alkali treatment is illustrated in Figure 2. The treated paddy straw with a fibre length of 3 to 5 mm with 0.5mm dia was found suitable for making geopolymer composites and was established in previous research[34]. The lignin, hemicellulose, and pectin in the raw paddy straw were intended to be dissolved by the alkali treatment with the NaOH solution. All the impurities were removed completely with this treatment. Further, this treatment helps break the bundles of fibres into fractions, producing more surface area and hence more contact between fibre and surrounding composites [6-8, 15, 16].

Raw Paddy straw

Shredded paddy straw

Paddy straw soaked with NaOH solution

FIGURE 2 The process of alkali treatment

Geopolymer Composite Preparation

The composites have been made using a variation of paddy straw (0%, 5%, 10%, 15%, and 20%), GGBS, and alkaline activator. The ratio of alkaline activator to GGBS was maintained as 0.7[31]. The details of the mix are presented in Table 3. This research used a mortar mixer to make slurry along with paddy straw fibres. In this process, the activators were reacted with binding material first and then filled with fibres[35, 36]. The blended slurry was poured into the cubic mould of size 50 mm x 50 mm x 50 mm and prism of size 160 mm x 40 mm x 40 mm for compression and flexural strength testing. Two pouring layers were adopted, and each layer was tamped 25 times to ensure proper compaction. The cast samples were allowed to be set for 24 h at ambient temperature and demolded for curing.

TABLE 3 Details of geopolymer composite mixes with varying parameters

Mix ID	GGBS (%)	Paddy straw (%)	Liquid binder ratio	Curing media
MP0	100	0	0.7	Intermittent
MP5	95	5	0.7	Intermittent
MP10	90	10	0.7	Intermittent
MP15	85	15	0.7	Intermittent
MP20	80	20	0.7	Intermittent

MP0	100	0	0.7	Heat
MP5	95	5	0.7	Heat
MP10	90	10	0.7	Heat
MP15	85	15	0.7	Heat
MP20	80	20	0.7	Heat
MP0	100	0	0.7	Saline
MP5	95	5	0.7	Saline
MP10	90	10	0.7	Saline
MP15	85	15	0.7	Saline
MP20	80	20	0.7	Saline

Curing

As per the previous research, the curing media influences the strength development of geopolymer composites[37]. Considering the curing media's aspects, this experimental work has been done with three different curing media. For the first media of curing, a set of samples were heat cured at 60 ^{0}C for 6h in a hot air oven. After heat curing, the samples were kept at ambient room temperature till the date of testing [31,38]. Intermittent curing was done by soaking the samples in normal water for 7 days and left to air cure for the remaining 21 days at ambient conditions[39]. The saline solution was prepared by dissolving 35 grams of NaCl with 1 litre of normal water. Based on the previous research, the samples were soaked in saline water for 28 days[40].

Fourier Transform Infrared Spectroscopy (FTIR) of Untreated and Treated paddy straw fibres

The chemical structure of untreated and treated paddy straw was studied with Fourier Transform Infrared Spectroscopy (FTIR) to identify the modified functional groups by the treatment. An FTIR spectrometer simultaneously collects high-resolution spectral data over a broad range, such as 400-

4000 cm^{-1}. The microstructural analysis procedure was followed from the previous research work [41].

Thermogravimetric Analysis of treated and untreated paddy straw

Thermo gravimetric analysis (TGA) has been employed to investigate the impact due to temperature and to predict the impact of thermal stability and degradation of untreated paddy straw fibre and treated paddy straw fibres. The paddy straw was shredded to have a fibre of length 3-5 mm with 0.5mm dia tested by TGA scan at 25°C to 1200°C under a heating rate of 2°C/ min. The inert atmosphere for this test was Nitrogen. The instrument model used for the study was NETZSCH STA 449F3. The untreated paddy straw weighed 2.171 mg in an AL-203 Crucible. During the entire heating operation, the mass loss of the material was investigated and recorded at regular time intervals.

Physical Properties of Geopolymer Composites

After mixing, a flow test was conducted in line with ASTM C230 to evaluate the workability of geopolymer composites. The flow test was performed by filling the moulds of size 50 mm with two layers of mortar 25mm thick on each layer. Tamping of geopolymer composites was carried out to obtain the proper compaction. After the complete compaction, the molds were removed, and the flow table was allowed to drop 25 times in 15sec, [31, and 42].

Geopolymer composites' initial and ultimate setting times have been measured in accordance with ASTM C191. The initial setting time was assessed by measuring the depth of the needle having a diameter of 1.13 mm allowed to fall under gravity, whereas the final setting time was measured by the time taken between the pouring of a mixture to solid surface penetration to a depth of 0.5 mm. The test was conducted at room temperature, and an optimum value was calculated.

The samples' dry bulk density was determined per ASTM C-642-13. The mass calculated the dry bulk densities to volume ratio, and density variation helps to identify the degree of geopolymerisation. A water absorption test was carried out in accordance with ASTM C1403-15, and the test results were recorded.

Mechanical Properties of Geopolymer Composites

The test setup followed by previous research work[43] assessed the specimens direct tensile strength. The 0.1 mm/min loading rate for the direct tensile test was achieved with a 100 kN Universal Instron testing instrument. The average direct tensile strengths of three samples were recorded for each curing condition and paddy straw %.

The direct compression test was conducted in accordance with ASTM C-109-20a. This experimental work was carried out with a compression testing machine of capacity 200 kN. The samples of size 50 mm x 50 mm x 50 mm were tested at 7 days, 14 days, and 28 days of casting. The 0.5 mm/min loading rate was applied until the sample reached the peak load. Three identical specimens from each mix were taken for testing, and the mean values of the samples were recorded.

The flexural test procedure was executed at ambient temperature in accordance with ASTM C 348. The samples from all the mix of size 160 mm x 40 mm x 40 mm were allowed for three-point bending. The bending test was performed with Instran 500 testing machine at a 0.5mm/min loading rate. All the specimens were kept at the orientation of the tensile surface perpendicular direction of lamination, and the maximum load under failure conditions was recorded.

EXPERIMENTAL RESULTS AND DISCUSSION

FTIR of Untreated and Treated Paddy straw fibres

Figure 3a displays the FTIR spectrum of untreated paddy straw fibres. The biomass sample contains a simple spectrum (5 or less absorption bands). The strongest bands are found between 1655cm^{-1} and 487cm^{-1} in the sample. The peaks were obtained at single bond area (2500-4000 cm^{-1}). The absence of a broad absorption band indicates that the material contains no hydrogen bonds. The absence of a sharp bond at approximately 3500 cm^{-1} demonstrates the absence of oxygen-related bonding. Between 2700 and 2800 cm^{-1}, no particular aldehyde peak has been identified. It was discovered that there was no triple bond region (2000–2500 cm^{-1}), indicating that the material lacked a C≡C bond. A sharp peak was seen in the double bond region (1500-2000 cm^{-1}), around 1654 cm^{-1}. This provides information about a carbonyl double bond, which can come from amides, ketones, aldehydes, esters, or carboxyl. Since a distinct peak may be found between 1630 and 1680 cm^{-1}, the anticipated peak for carbonyl should come from amide. The peak in 1280 cm^{-1} indicates the existence of organic phosphates (1350-1250 cm^{-1}) in the sample. Phosphate (1100-1000 cm-1) and silicate (110-090 cm-1) ion content can be deduced from the 1022 cm-1 peak. The presence of methylene is indicated by the appearance of a peak at 748 cm-1 (750-720 cm-1). The presence of Aryl disulfides (500-430 cm-1) and Polysulfides (500-470 cm-1) is shown by the peak at 487 cm-1. The FTIR spectrum of the treated paddy straw fibres is shown in Figure. 3b indicates the altered chemical composition of the fibres. From the test findings, FTIR reveals that the biomass sample of treated paddy straw has a simple spectrum (5 or less absorption bands). The strongest bands were found between 3643.53cm^{-1} and 777.31cm^{-1} in the sample. A single bond region was formed between 2500 and 4000 cm^{-1}. The major alcohol, OH groups, are represented by the peak at 3643 cm-1. The material has no C≡C bond, as evidenced by detecting a triple bond area (2000–2500 cm^{-1}). A sharp peak was found in the double bond region (1500-2000 cm^{-1}), around 1761 cm^{-1}. This indicates the presence of carbonyl compounds like amide, ketone, acyl halide group, etc. Organic

phosphates (1350-1250 cm-1) are present in the sample, as seen by the 1344 cm-1 peak. The presence of aromatic phosphates (995-850 cm-1) is shown by the 905 cm-1 peak, while the presence of the C-Cl stretch is indicated by the 777 cm-1 peak. The decline occurs due to the removal of hemicellulosis from the fibre surface, brought about by alkaline treatment with NaOH solution. Analysis of the FT-IR spectra reveals that the treated paddy straw fibre surface has undergone a chemical change. In relation to the lignin component, it has been shown that the hemicellulose components detached during the alkali treatment process.

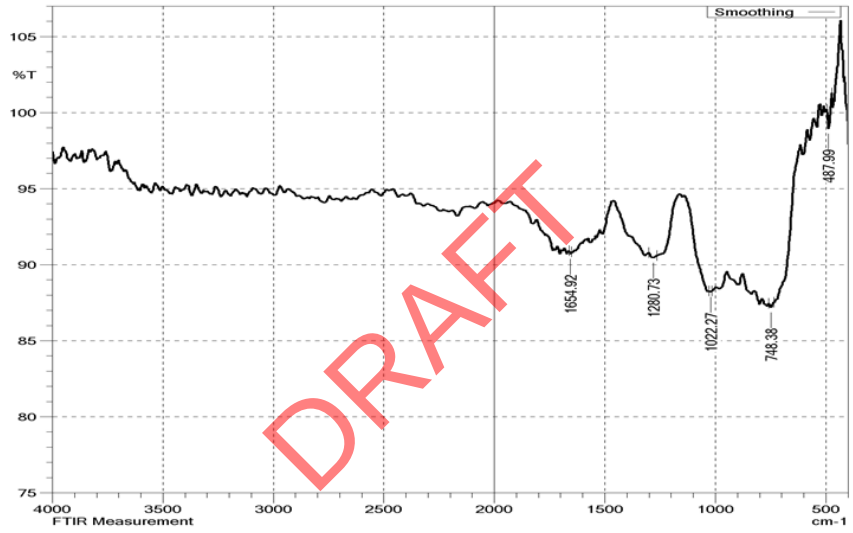

FIGURE 3a FTIR spectrum of Untreated paddy straw fibre

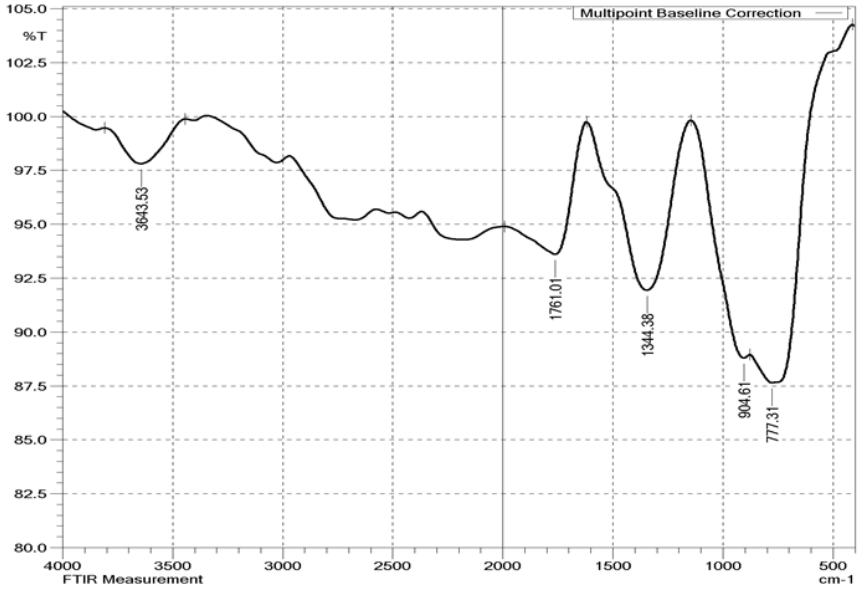

FIGURE 3b FTIR spectrum of Treated paddy straw fibre

Thermo gravimetric Analysis (TGA) of Untreated and Treated Paddy Straw

Materials made up of cellulose are extremely temperature sensitive. Studying the thermal characteristics of agricultural paddy straw fibres is crucial to determining how well they will work in reinforced geopolymer composites because many geopolymer materials require processing temperatures higher than 100 C. The test results of TGA for untreated and treated paddy straw fibres have been plotted for Mass Vs. The temperature is shown in Figure 4a, b. The mass of the sample is represented in '%' along the Y axis, and the temperature is represented in '°C' along the X axis. The graph for the untreated paddy straw illustrates that thermal degradation occurred in three major stages: Removal of moisture, Loss of volatile matter, and Loss of fixed carbon. From the results in the 1st Stage, the 3.04% mass loss indicates the loss of moisture content from the untreated paddy straw. 2nd Stage has a mass loss of 35.97%. In this Stage, a sudden drop in the TGA curve shows the importance of this Stage. The major volatile matter removed in this 3rd Stage has a mass loss of 6.17%, indicating the combustion of fixed carbon. A gain in mass occurred after

253 the 3rd Stage. This indicates the Oxidation process. The cleavage of a bond must have occurred in
254 the 2nd Stage.

255 The obtained test values of treated paddy straw, shown in Figure 4b, show that the degradation
256 temperature rises significantly after treatment. Additionally, as the treatment duration is extended,
257 the deterioration temperature rises; the same was indicated by previous research work also[44]. The
258 treated paddy straw fibre decomposes from 235-255°C. This shows that the treated residues have a
259 higher degree of thermal stability. The carbonaceous elements in the paddy straw under nitrogen
260 atmosphere are indicated by the fibre residue that remains after heating of 530°C[45]. The residue in
261 the fibres obtained after treatments were relatively low because calcium oxalate crystals of lignin
262 and other ash sources were removed during the high-pressure and temperature procedure. These
263 results suggest that hemicellulose and lignin were partially removed, leading to a decreased residual
264 mass of paddy straw fibres, which increased the temperature at which they decomposed. All these
265 points to a noticeable improvement in the thermal resistance of treated paddy straw fibres. These
266 outcomes are remarkably in line with those of the FTIR analysis.

267 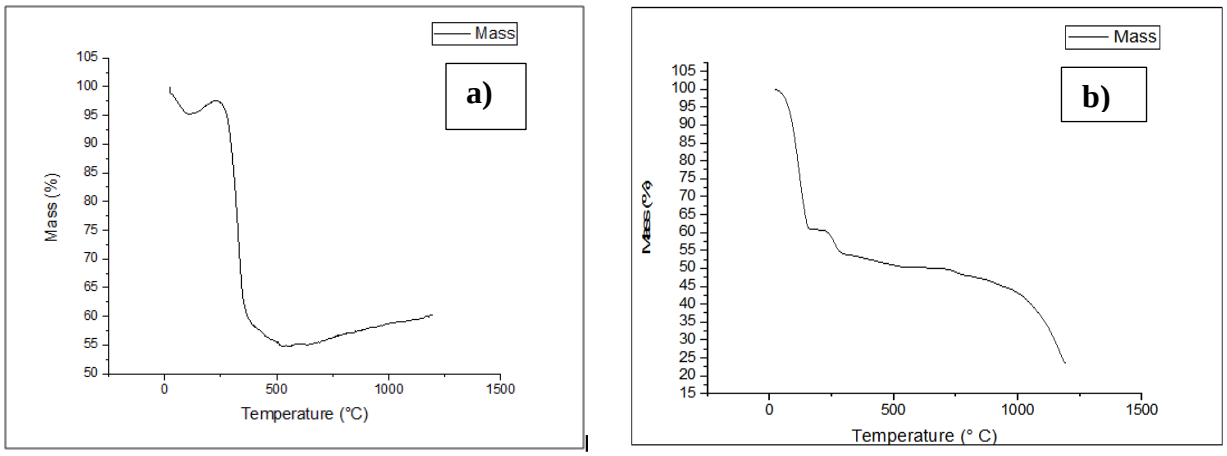

268 **FIGURE 4a, b** Plot of Temperature Vs. Mass for Untreated Paddy straw sample and Treated paddy
269 straw sample, respectively

Microstructural properties of geopolymer composites

Typical SEM images in Figure 5 a, b, and c illustrate the microstructural properties of geopolymer composites cured under different media. For comparison, Figure 5 a, b, and c are selected under different curing conditions with the same magnification (100µm). It was discovered from the SEM images that the morphology of each curing media varied from one another. Each curing media had different degrees of polymerization. As a result, the finished product is a composite made of non-reacted raw materials and non-activated crystalline particles incorporated as fillers in a matrix of cementitious geopolymer. The sample cured under saline water exhibited color contrast among the darker inside core and lighter outside layer. Subsequent sections will provide more information on the microstructural characterization among various curing media.

The morphological natures of synthesized geopolymer under different curing media are presented in Figure 5. The samples that were cured in saline water appear (Figure 5c) to have a more uniform geopolymer binder than those that were cured in the other two media (Figure 5 a, b). High homogeneity and continuous matrix are closely linked to increased cementitious geopolymer binder, which raises unconfined compressive strength. Additional characteristics significantly found in SEM images were the appearance of micro cracks. The potential cause of microcracks formation is air-drying and curing of geopolymers. Even though their contribution is minor, the extensive microcracks in the geopolymeric matrix can noticeably impact strength.

In Figure 6, the microstructure of the synthesized geopolymer particle cured under Intermittent, Heat and saline water like that observed in Figure 5. The images make it clear that the degree of polymerization occurred on the samples in various curing environments. The fact that the particles in Figure. 6c appears to have fully reacted compared to Figure. 6a and 6b suggests that total

polymerization happened on saline-cured samples rather than the other two media of curing. Further research should be done to understand better the relationships between density, porosity, and cracks.

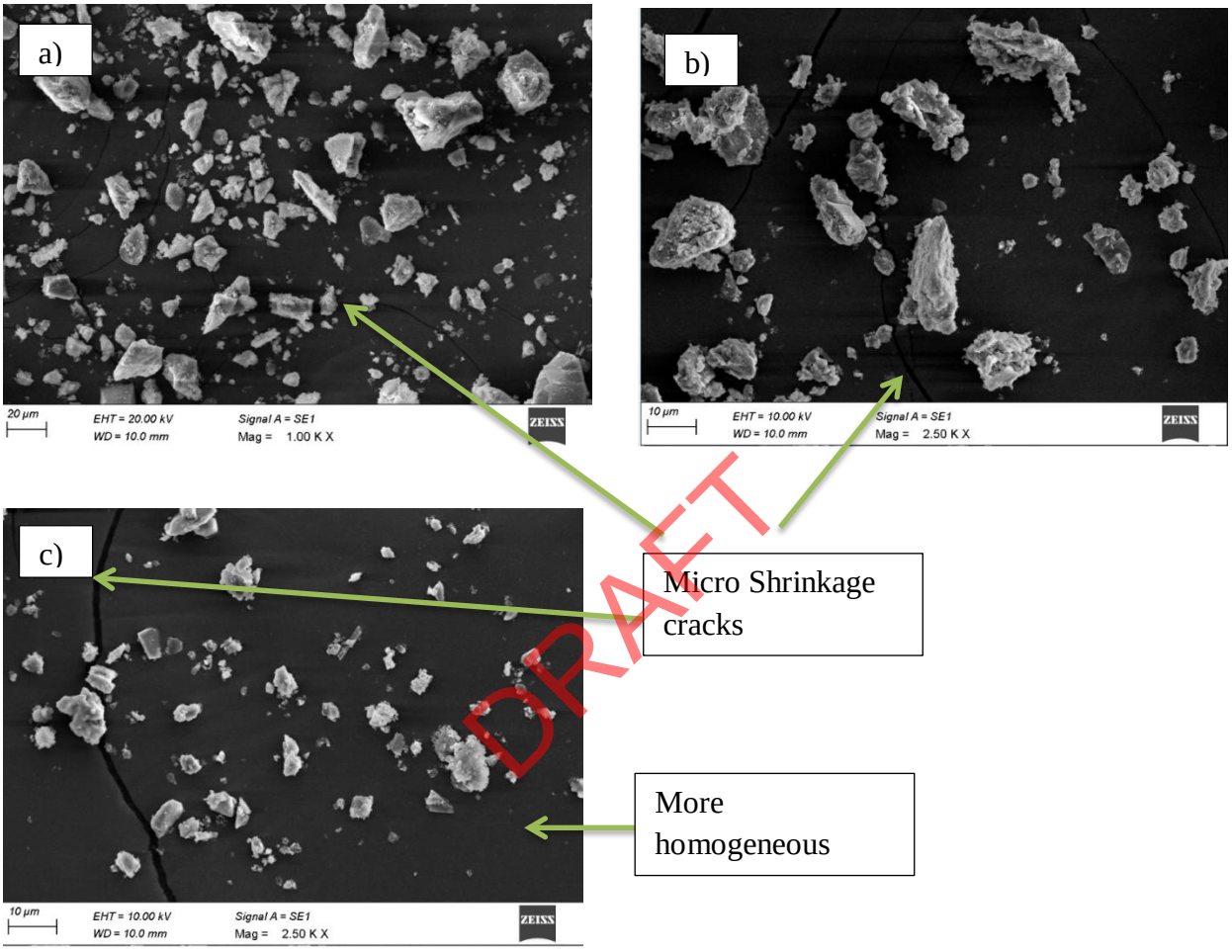

FIGURE 5 Morphological structure of synthesized geopolymer at 100µm and under a) Intermittent curing, b) Heat curing, c) Saline water curing

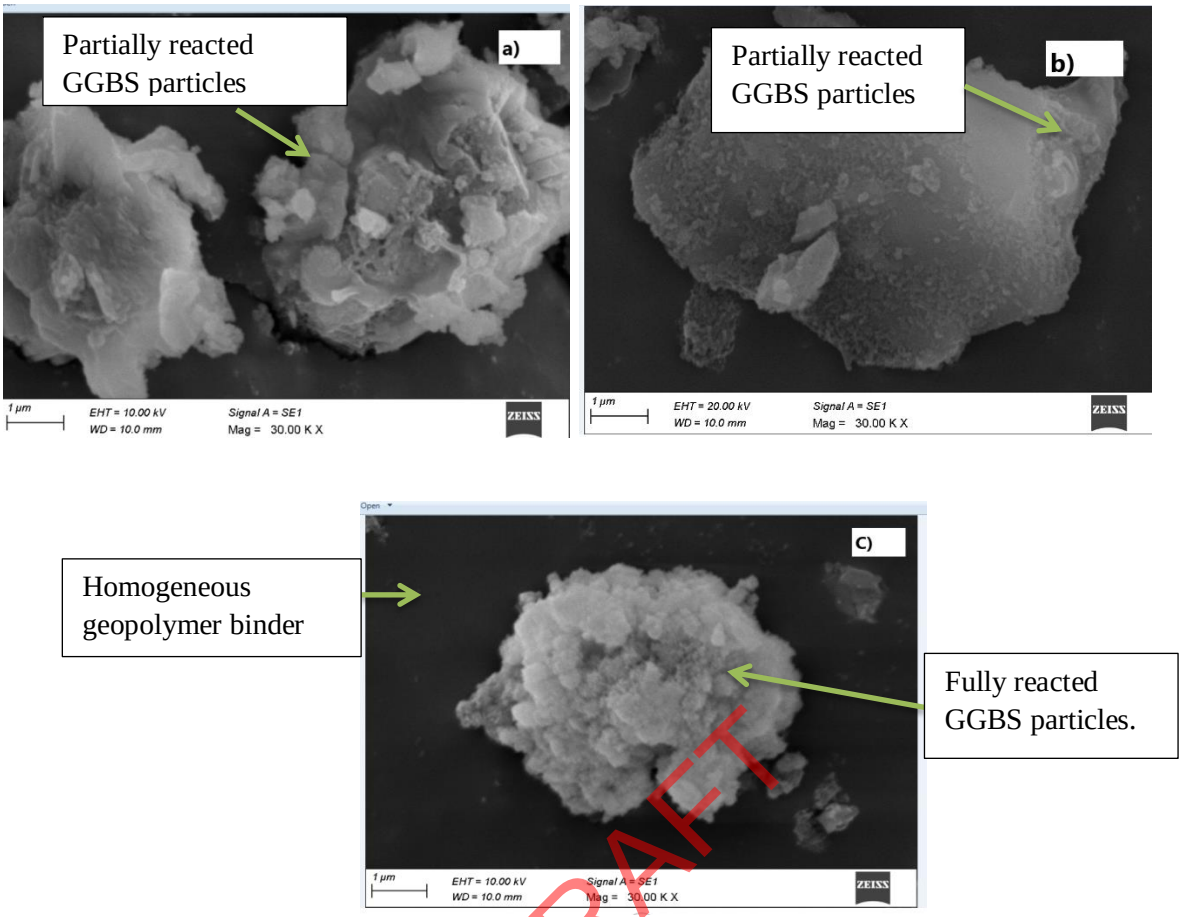

FIGURE 6 Microstructural overview of synthesized geopolymer at 1µm scale and under a) Intermittent curing, b) Heat curing, c) Saline water curing

Fresh Properties of Geopolymer Composites

The test result obtained from the flow table test was plotted as scattered points in Figure 7. The flow diameter for the mix ID MP0, MP5, MP10, MP15, and MP20 was 93 mm, 81 mm, 79 mm, 73 mm, and 70 mm, respectively. The Figure demonstrates the increase in the percentage of paddy straw content reduces the workability. Due to its very porous fibre structure, paddy straw has the potential to absorb more water from the geopolymer slurry, resulting in poor workability.

The initial and final setting time was plotted in Figure. 8 as scattered points. The test results illustrate a reduction of the initial and final setting time of sample MP20 at 50% and 44.7%, respectively. A linear relationship was established between the percentage of paddy straw addition and the setting time of composites. Due to the high-water absorption capacity of paddy straw, it absorbs more water from the composites and accelerates the setting process, which intern reduces the setting time.

Dry bulk densities for a varying proportion of paddy straw with varying curing media were plotted in Figure 9 after 28 days of curing and drying. Adding paddy straw by 0%-20% reduces its density by 40.42%. This graph reflects that the increase in paddy straw percentage reduces composites' density. An interesting fact found from the graph is that, while considering curing media saline cured sample exhibited denser composites (nearly 9.3% high) than the other two cured samples. The reason behind that there might be less leaching, and more geopolymerisation takes place on saline curing media. These findings helped develop a lightweight geopolymer under a suitable curing media supported by the previous researcher[46].

A water absorption test was performed for the samples cured under intermittent, heat, and saline environments at 2 h, 24 h, and 48 h, and the test results were plotted in Figure 10. Among all the curing media, the intermittent curing media attained the maximum water absorption percentage of nearly 19.3% at 48 h, whereas the saline-cured sample reached only 11%. It was evident that the high polymerization of the saline-cured sample exhibited a less porous structure. As a result of a less porous structure, water absorption capacity was significantly reduced, and hence improvement in strength was achieved.

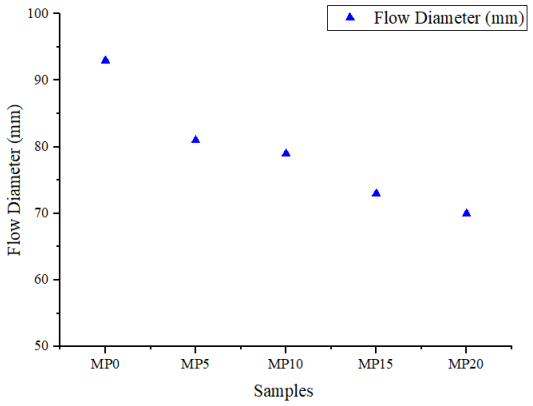

330

FIGURE. 7 Flowability

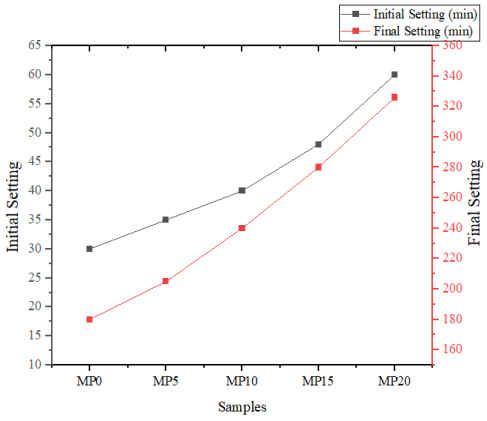

FIGURE. 8 Initial & Final Setting Time

331

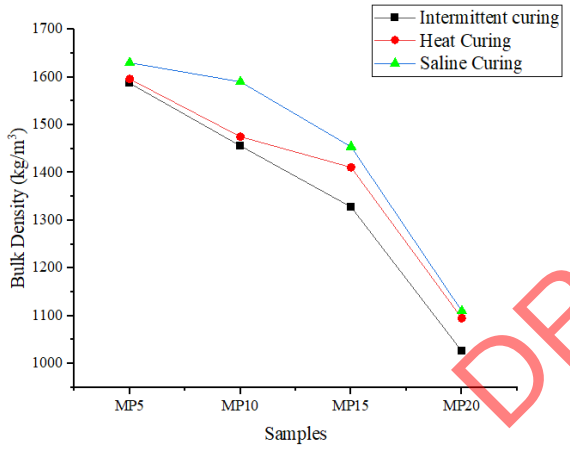

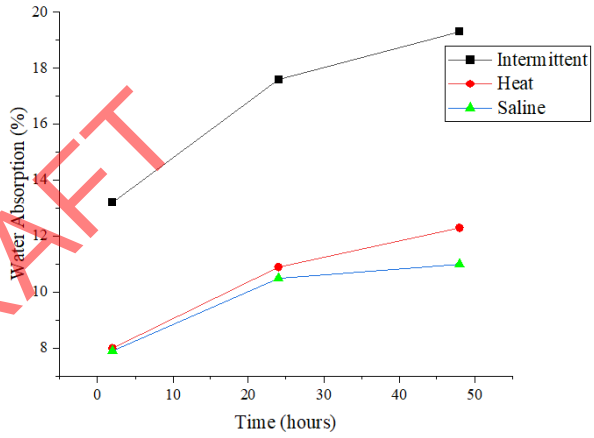

332

333 **FIGURE 9** Dry bulk density

FIGURE 10. Percentage of water absorption

334 **Mechanical Properties of Geopolymer Composites**

335 The direct tensile strength of samples subjected to various curing media with varying percentages
336 of paddy straw is presented in Figure 11. The peak tensile strength (1.6 MPa) was obtained on
337 saline-cured M15 samples, and the values were gradually reduced to 1.4 MPa for the samples
338 MP20. The Figure illustrates the increasing percentage of paddy straw content from 0%-15%
339 improves the tensile strength, and the reduction occurred for the samples at 20% paddy straw
340 addition. The tensile strength of the sample MP0 (without paddy straw) is negligible or less (0.15

MPa) compared to the sample MP15. Further, the saline curing media contributes to the enhancement of tensile strength by 45.5% from the other two curing media for MP15 samples. High polymerization increases the tensile properties of saline-cured samples could be the root cause of strength improvement.

To differentiate the strength variation with the percentage of paddy straw and various curing media, the graph is plotted against compressive and tensile strength, as shown in Figure 12. The Figure depicts the decline of compressive strength with the increase in paddy straw addition. It is evident from the graph that the saline-cured samples show a greater value. Saline-cured MP0 attained the peak value of 79 MPa, whereas MP20 attained only 9.1 MPa. Nearly 88.6% of compressive strength getting reduced by adding 20% paddy straw. While discussing the curing media, saline-cured samples yielded nearly 12.85 % higher value than the other two curing media. From the test results, it was ascertained that paddy straw variation and curing media played a vital role in strength development.

A flexural strength test was conducted to investigate the resistance against deformation loads, and the test results are plotted in Figure 12. The peak flexural strength yielded at MP15 samples is 4.25 MPa, and the lowest value obtained for the samples MP0 is 3 MPa. After attaining the peak value at MP15, the value is reduced for the further addition of paddy straw. The declination after the peak indicates that excess paddy straw reduces the bond strength while testing. These test values provide knowledge about the variation of paddy straw and flexural strength development. According to a prior report, the primary factor in developing flexural strength was binding between the fibre and the surrounding composites.[47-50]. The same scenario applies to cellulose-based fibres, as the paddy straw-reinforced geopolymer composites increase their strength due to the efficient bonding between fibre and the surrounding matrix. The strength variation within the same mixture was

observed with different curing media. The saline cured sample yielded 21.2% maximum flexural strength than the other two curing media. With the above findings, the addition of paddy straw has a positive impact on flexural strength development.

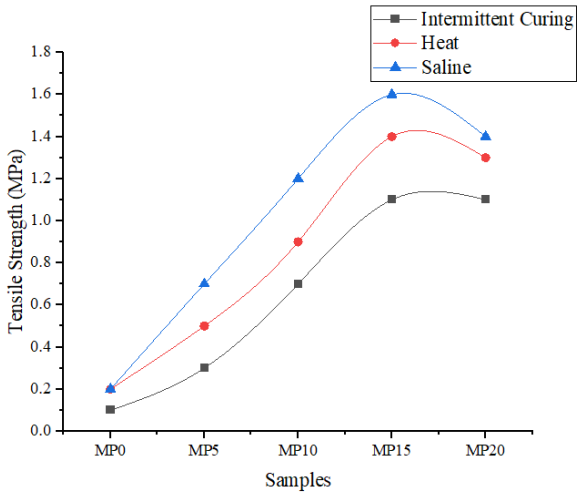

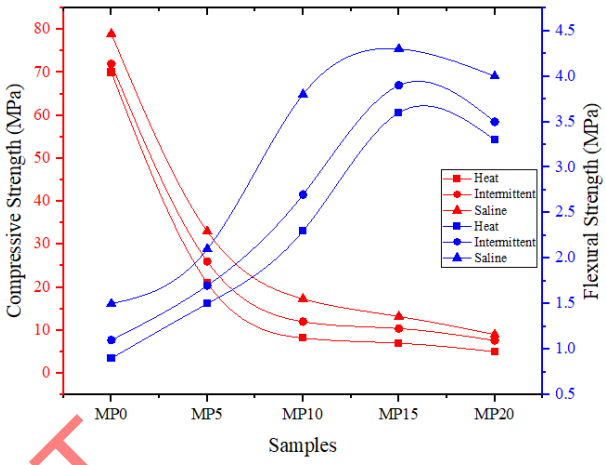

FIGURE 11 Tensile strength

FIGURE 12 Compressive strength

CONCLUSIONS

This experimental study illustrates the impact of various curing media and paddy straw addition on the properties of lightweight geopolymer composites. From the test findings, adding the curing media and paddy straw might provide a wide range of geopolymer properties and change in density, compressive strength, tensile strength, and flexural strength. The maximum reduction of workability, setting time, and density achieved for 20% addition of paddy straw is 24.7%, 44.7%, and 40.42%, respectively. As the density and compressive strength are directly proportional, it is evident that the reduction of compressive strength to the addition of paddy straw. The results showed that when 20% paddy straw was added, the compressive strength dropped by about 88.6%. While discussing the flexural strength, there was a positive sign in strength, nearly 65.11% improvement for the 15% addition of paddy straw, and the value declined by 15-20%. The tensile

strength rises its value by 60% for a 15% increment of paddy straw and is reduced after attaining the peak strength.

While considering the contribution of paddy straw to geopolymer, it is noteworthy to highlight the role of curing media on the properties. A wide range of property changes was found among the curing media. The density of geopolymer composites improved its value by 9.3% than the other two curing media. As the density and water absorption are indirectly proportional, lower water absorption was found for saline-cured samples. Nearly 12.85% compressive strength improvement was found for the saline-cured sample than the intermittent and heat-cured samples. The changes in strength obtained for tensile and flexure were 45.5% and 21.2%, respectively. High polymerized structure at saline cured sample exhibits the strong link between treated paddy straw and the geopolymer matrix, which increases overall performance.

The FTIR findings reveal that the treated paddy straw fibre surface has changed chemically. Hemicelluloses and lignin components from the fibre surface detached during the alkali treatment. TGA report exhibits that paddy straw fibres have excellent thermal stability characteristics and a rise in thermal degradation temperature, making them promising materials for utilization in geopolymer composites. SEM images of Synthesized geopolymer indicate that total geopolymerization happened on saline-cured samples rather than the other two curing media. High homogeneity and continuous matrix are closely linked to increased cementitious geopolymer binder, which raises unconfined compressive strength, tensile strength, and flexural strength.

From the above discussion, both the curing media and paddy straw variation influence geopolymer composites' properties. And hence, the lightweight geopolymer cured under saline media is viable alternative construction material as it possesses higher mechanical properties than others. The

optimal mix design developed for ambient curing must be reassessed and altered for in-situ casting under various curing media. Such adjustments include changing the aluminosilicate source and varying saline and alkali solutions concentrations.

Authors Contribution:

All authors have equal contribution in the article:

Data Availability:

Data will be available by sending reasonable request to corresponding author:

Conflict of Interest:

Authors declare no conflict of interests

Funding :

There is no funding is taken for the current manuscript

This material is the authors' own original work, which has not been previously published elsewhere.

Reference:

1. Andreae, M.O., Merlet, P.: Emission of trace gases and aerosols from biomass burning. Global Biogeochem. Cycles. 15, 955–966 (2001)

2. Kadam, K.L., Forrest, L.H., Jacobson, W.A.: Rice straw as a lignocellulosic resource: collection, processing, transportation, and environmental aspects. Biomass and Bioenergy. 18, 369–389 (2000)

3. Chen, J., Elbashiry, E.M.A., Yu, T., Ren, Y., Guo, Z., Liu, S.: Research progress of wheat straw and rice straw cement-based building materials in China. Mag. Concr. Res. 70, 84–95 (2018)

4. Morsy, M.I.N.: Properties of rice straw cementitious composite, (2011)

5. Ataie, F.: Influence of rice straw fibres on concrete strength and drying shrinkage. Sustainability. 10, 2445 (2018)

6. Pacheco-Torgal, F., Jalali, S.: Cementitious building materials reinforced with vegetable fibres: A review. Constr. Build. Mater. 25, 575–581 (2011)

7. Sedan, D., Pagnoux, C., Smith, A., Chotard, T.: Mechanical properties of hemp fibre reinforced cement: Influence of the fibre/matrix interaction. J. Eur. Ceram. Soc. 28, 183–192 (2008)

8. Mishira, S., Mohanty, A.K., Drzal, L.T., Misra, M., Hinrichsen, G.A.: Review on pineapple leaf fibres, sisal fibres and their biocompositers. Macromol. Mater. Eng. 289, 955–974 (2004)

9. Lim, S.K., Tan, C.S., Lim, O.Y., Lee, Y.L.: Fresh and hardened properties of lightweight foamed concrete with palm oil fuel ash as filler. Constr. Build. Mater. 46, 39–47 (2013)

10. Petrillo, A., Cioffi, R., De Felice, F., Colangelo, F., Borrelli, C.: An environmental evaluation: a comparison between geopolymer and OPC concrete paving blocks manufacturing process in Italy. Environ. Prog. Sustain. Energy. 35, 1699–1708 (2016)

11. Davidovits, J.: Geopolymers: inorganic polymeric new materials. J. Therm. Anal. Calorim. 37, 1633–1656 (1991)

12. Davidovits, J.: Global warming impact on the cement and aggregates industries. World Resour. Rev. 6, 263–278 (1994)

13. Davidovits, J.: Inorganic polymeric new materials. J. Therm. Anal. 37, (1991)

14. Davidovits, J.: Properties of geopolymer cements. In: First international conference on alkaline cements and concretes. pp. 131–149. Kiev State Technical University Kiev, Ukraine (1994)

15. Davidovits, J., Sawyer, J.L.: Early high-strength mineral polymer, (1985)

16. Duxson, P., Fernández-Jiménez, A., Provis, J.L., Lukey, G.C., Palomo, A., van Deventer, J.S.J.: Geopolymer technology: the current state of the art. J. Mater. Sci. 42, 2917–2933 (2007)

17. Siddiqui, K.S.: Strength and durability of low-calcium fly ash-based geopolymer concrete. Final Year Honours Diss. Univ. West. Aust. Perth. (2007)

18. Gourley, J.T., Johnson, G.B.: Developments in geopolymer precast concrete. In: World congress geopolymer. pp. 139–143. Geopolymer Institute Saint-Quentin, France (2005)

19. Singh, N.B., Middendorf, B.: Geopolymers as an alternative to Portland cement: An overview. Constr. Build. Mater. 237, 117455 (2020)

20. Suwan, T., Fan, M.: Influence of OPC replacement and manufacturing procedures on the properties of self-cured geopolymer. Constr. Build. Mater. 73, 551–561 (2014)

21. Dimas, D., Giannopoulou, I., Panias, D.: Polymerization in sodium silicate solutions: a fundamental process in geopolymerization technology. J. Mater. Sci. 44, 3719–3730 (2009)

22. Kirschner, A., Harmuth, H.: Investigation of geopolymer binders with respect to their application for building materials. Ceramics-silikaty. 48, 117–120 (2004)

23. Mallikarjuna Rao, G., Gunneswara Rao, T.D.: Final setting time and compressive strength of fly ash and GGBS-based geopolymer paste and mortar. Arab. J. Sci. Eng. 40, 3067–3074 (2015)

24. Mangat, P., Lambert, P.: Sustainability of alkali-activated cementitious materials and geopolymers. In: Sustainability of construction materials. pp. 459–476. Elsevier (2016)

25. Shi, C., Roy, D., Krivenko, P.: Alkali-activated cements and concretes. CRC press (2003)

26. Van Deventer, J.S.J., Provis, J.L.: Alkali-Activated Materials: State-of-the-Art Report, RILEM TC 224-AAM, (2014)

27. Talling, B., Krivenko, P.: Blast furnace slag-the ultimate binder. In: Waste materials used in concrete manufacturing. pp. 235–289. Elsevier (1996)

28. Lee, W.K.W., Van Deventer, J.S.J.: The effects of inorganic salt contamination on the strength and durability of geopolymers. Colloids Surfaces A Physicochem. Eng. Asp. 211, 115–126 (2002)

29. Giasuddin, H.M., Sanjayan, J.G., Ranjith, P.G.: Strength of geopolymer cured in saline water in ambient conditions. Fuel. 107, 34–39 (2013)

30. Thirumakal, P., Nasvi, M.C.M., Sinthulan, K.: Comparison of mechanical behaviour of geopolymer and OPC-based well cement cured in saline water. SN Appl. Sci. 2, 1–17 (2020)

31. Wallah, S., Rangan, B.V.: Low-calcium fly ash-based geopolymer concrete: long-term

properties. (2006)

32. Zhu, S., Wu, Y., Yu, Z., Liao, J., Zhang, Y.: Pretreatment by microwave/alkali of rice straw and its enzymic hydrolysis. Process Biochem. 40, 3082–3086 (2005)

33. Zhang, Q., Cai, W.: Enzymatic hydrolysis of alkali-pretreated rice straw by Trichoderma reesei ZM4-F3. Biomass and Bioenergy. 32, 1130–1135 (2008)

34. Korniejenko, K., Frączek, E., Pytlak, E., Adamski, M.: Mechanical properties of geopolymer composites reinforced with natural fibres. Procedia Eng. 151, 388–393 (2016)

35. Tan, J., Lu, W., Huang, Y., Wei, S., Xuan, X., Liu, L., Zheng, G.: Preliminary study on compatibility of metakaolin-based geopolymer paste with plant fibres. Constr. Build. Mater. 225, 772–775 (2019)

36. He, J., Jie, Y., Zhang, J., Yu, Y., Zhang, G.: Synthesis and characterization of red mud and rice husk ash-based geopolymer composites. Cem. Concr. Compos. 37, 108–118 (2013)

37. Zhang, P., Zheng, Y., Wang, K., Zhang, J.: A review on properties of fresh and hardened geopolymer mortar. Compos. Part B Eng. 152, 79–95 (2018)

38. Hardjito, D., Wallah, S.E., Sumajouw, D.M.J., Rangan, B.V.: On the development of fly ash-based geopolymer concrete. Mater. J. 101, 467–472 (2004)

39. El-Hassan, H., Ismail, N.: Effect of process parameters on the performance of fly ash/GGBS blended geopolymer composites. J. Sustain. Cem. Mater. 7, 122–140 (2018)

40. Ge, X., Guo, B., Guo, D., Tao, M., Zhang, G.: Effects of pre-setting chemical exchanges on geopolymers cast in saline waters. Constr. Build. Mater. 308, 125020 (2021)

41. Ismail, I., Bernal, S.A., Provis, J.L., San Nicolas, R., Hamdan, S., van Deventer, J.S.J.: Modification of phase evolution in alkali-activated blast furnace slag by the incorporation of fly ash. Cem. Concr. Compos. 45, 125–135 (2014)

42. Hardjito, D.: Studies of fly ash-based geopolymer concrete, (2005)

43. Alhussainy, F., Hasan, H.A., Rogic, S., Sheikh, M.N., Hadi, M.N.S.: Direct tensile testing of self-compacting concrete. Constr. Build. Mater. 112, 903–906 (2016)

44. Chen, X., Yu, J., Zhang, Z., Lu, C.: Study on structure and thermal stability properties of cellulose fibres from rice straw. Carbohydr. Polym. 85, 245–250 (2011)

45. Xiao, B., Sun, X., Sun, R.: Chemical, structural, and thermal characterizations of alkali-soluble lignins and hemicelluloses, and cellulose from maize stems, rye straw, and rice straw. Polym. Degrad. Stab. 74, 307–319 (2001)

46. Sales, A., De Souza, F.R., Dos Santos, W.N., Zimer, A.M., Almeida, F. do C.R.: Lightweight composite concrete produced with water treatment sludge and sawdust: Thermal properties and potential application. Constr. Build. Mater. 24, 2446–2453 (2010)

47. Browning, J., Darwin, D., Reynolds, D., Pendergrass, B.: Lightweight aggregate as internal curing agent to limit concrete shrinkage. Presented at the (2011)

48. Abu-Lebdeh, T., Hamoush, S., Heard, W., Zornig, B.: Effect of matrix strength on pullout behavior of steel fibre reinforced very-high strength concrete composites. Constr. Build. Mater. 25, 39–46 (2011)

49. Naaman, A.E., Najm, H.: Bond-slip mechanisms of steel fibres in concrete. Mater. J. 88, 135–145 (1991)

523 50. Kim, D.J., El-Tawil, S., Naaman, A.E.: Effect of matrix strength on pullout behavior of high-
524 strength deformed steel fibres. Spec. Publ. 272, 135–150 (2010)

525

526